(NASA-TM-83814) ELECTROCHEMICAL MODELS FOR THE DISCHARGE CHARACTERISTICS OF THE NICKEL CADMIUM CELL (NASA) 19 p HC A02/MF A01
CSCL 10C
N82-12569
Unclas
G3/44 03299

NASA

Technical Memorandum **83814**

Electrochemical Models for the Discharge Characteristics of the Nickel–Cadmium Cell

AUGUST 1981

National Aeronautics and
Space Administration

Goddard Space Flight Center
Greenbelt, Maryland 20771

ELECTROCHEMICAL MODELS FOR THE DISCHARGE CHARACTERISTICS OF THE NICKEL- CADMIUM CELL

Michael S. Spritzer

NASA/ASEE Summer Faculty Fellow
1981

Department of Chemistry
Villanova University
Villanova, PA

August 1981

Goddard Space Flight Center
Greenbelt, Maryland

CONTENTS

ILLUSTRATIONS

TABLES

ELECTROCHEMICAL MODELS FOR THE DISCHARGE CHARACTERISTICS OF THE NICKEL-CADMIUM CELL

INTRODUCTION

Basic electrochemical principles were applied to the sealed nickel-cadmium cell in an effort to describe its behavior and to predict its operating characteristics. An essentially thermodynamic approach was taken to arrive at several related but different equations describing its discharge.

This investigation represents but one phase in an extensive effort to characterize the behavior of the nickel-cadmium cell. The study presented here does not incorporate such operational variables as depth of discharge, long-term aging, repeated cycling, preconditioning, rate of charge, etc. but merely considers the potential-time characteristics of a "preconditioned," fully charged cell discharged at constant current. Constant current operation was selected because it is simpler to describe and to facilitate comparison with the long-term experimental data which have been accumulated in that mode (1).

MODEL I. SIMPLE THERMODYNAMIC MODEL

The reaction taking place at the positive electrode of a nickel-cadmium cell, i.e., the cathode during discharge, is usually taken to be (2,3):

$$NiOOH + H_2O + e \rightleftharpoons Ni(OH)_2 + OH^- \tag{1}$$

The Nernst equation corresponding to this reaction is

$$E_{pos} = E^o_{pos} + \frac{RT}{nF} \ln \frac{a_{NiOOH}\, a_{H_2O}}{a_{Ni(OH)_2}\, a_{OH^-}} \tag{2a}$$

where R is the gas law constant, F the faraday, n the number of electrons, and T the absolute temperature. Upon rearranging terms,

$$E_{pos} = E^o_{pos} + \frac{RT}{F} \ln \frac{a_{NiOOH}}{a_{Ni(OH)_2}} + \frac{RT}{F} \ln a_{H_2O} - \frac{RT}{F} \ln a_{OH^-} \tag{2b}$$

At the negative electrode the reaction is (2)

$$Cd(OH)_2 + 2e \rightleftharpoons Cd + 2\,OH^- \tag{3}$$

The corresponding Nernst equation is

$$E_{neg} = E^{o}_{neg} + \frac{RT}{2F} \ln \frac{a_{Cd(OH)_2}}{a_{Cd}\, a^{2}_{OH^-}} \tag{4a}$$

or, upon rearranging

$$E_{neg} = E^{o}_{neg} + \frac{RT}{2F} \ln \frac{a_{Cd(OH)_2}}{a_{Cd}} - \frac{RT}{F} \ln a_{OH^-} \tag{4b}$$

The Nernst equation for the net cell reaction would then be given by $E_{cell} = E_{pos} - E_{neg}$, or

$$E_{cell} = E^{o}_{pos} - E^{o}_{neg} + \frac{RT}{F} \ln \frac{a_{NiOOH}}{a_{Ni(OH)_2}} - \frac{RT}{2F} \ln \frac{a_{Cd(OH)_2}}{a_{Cd}} + \frac{RT}{F} \ln a_{H_2O} \tag{5}$$

Now let us make the following assumptions:

(a) The Cd and the $Cd(OH)_2$ at the negative electrode appear as separate solid phases so that $a_{Cd} = a_{Cd(OH)_2} = 1$

(b) The NiOOH and $Ni(OH)_2$ at the positive electrode are present in a single phase, i.e., a solid solution.

Barnard, Randell and Tye (4,5) have presented evidence in support of this second hypothesis. Under these conditions the activities of NiOOH and $Ni(OH)_2$ would not be unity but could be expressed as their respective mole fractions:

$$a_{NiOOH} = X_{NiOOH} \text{ and } a_{Ni(OH)_2} = X_{Ni(OH)_2} .$$

If NiOOH and $Ni(OH)_2$ are the only species present in the solid solution, then

$$X_{NiOOH} + X_{Ni(OH)_2} = 1 .$$

Representing the mole fraction of $Ni(OH)_2$ by X then the mole fraction of NiOOH would be 1 - X. The quantity X may also represent the state of discharge, e.g., X = 0 corresponds to the fully charged material and X = 1 to the fully discharged. In addition, if one combines the term involving activity of water and the standard potentials into a formal cell potential, $E^{o'}$, then the Nernst equation has the form

$$E_{cell} = E^{o'}_{cell} + \frac{RT}{F} \ln \left(\frac{1-X}{X} \right) \tag{6a}$$

Under conditions of current flow the cell resistance must be taken into account so that the discharge curve will have the form

$$E = E^{o'} + \frac{RT}{F} \ell n \left(\frac{1-X}{X}\right) - i R_0 \qquad (6b)$$

where i is the total current, R_o is the cell resistance and X is the fraction of discharge.

The formal potential for the $Cd(OH)_2/Cd$ system is reported (2) as - 0.899 volts vs. Hg/HgO, and that for the $NiOOH/Ni(OH)_2$ system as 0.395 volts vs. Hg/HgO (2). Thus the formal potential for the net cell reaction is 0.395 + 0.899 = 1.294 volts, and the discharge equation becomes

$$E = 1.294 + \frac{RT}{F} \ell n \left(\frac{1-X}{X}\right) - i R_0 \qquad (7)$$

A calculated curve based on equation 7 is shown in Figure 1. An experimental curve obtained during a capacity test in the Crane series of nickel-cadmium battery tests (1) is shown for comparison. The cell resistance was calculated from the experimental potential at 50% discharge. Agreement with the experimental data is not very good. Further discussion of the errors will be presented later.

MODEL II. MODIFIED THERMODYNAMIC MODEL

Barnard, Randell and Tye (5) have described nickel hydroxide electrodes based on evaluation of the free energy of mixing two species in solid solution. The total free energy of the system is expressed as the sum of the free energy of reaction and the free energy of mixing. In addition, a so-called "excess energy" term is included to account for interactions between the species in the solid. As a result of their treatment, they arrived at an expression for the potential of the nickel hydroxide system:

$$E_{Ni} = E^{o}_{Ni} + \frac{RT}{nF} \ell n \left(\frac{1-X}{X}\right) + \frac{RT}{nF} \left(\frac{A}{RT}\right) (2X-1) \qquad (8a)$$

A value of A/RT = 0 represents "ideal" behavior and, in fact, corresponds to the simple thermodynamic approach of Model I. Values of A/RT = 1 or -1 represent respectively positive and negative deviation from ideality. The case where A/RT = 2 corresponds to the borderline between a single-phase and a two-phase system. The reader is urged to consult the original paper for details.

When this modified thermodynamic approach is included, the equation for a Ni-Cd discharge curve becomes

$$E = 1.294 + \frac{RT}{F} \ell n \left(\frac{1-X}{X}\right) + \frac{RT}{F} K (2X-1) - i R_0 \qquad (8b)$$

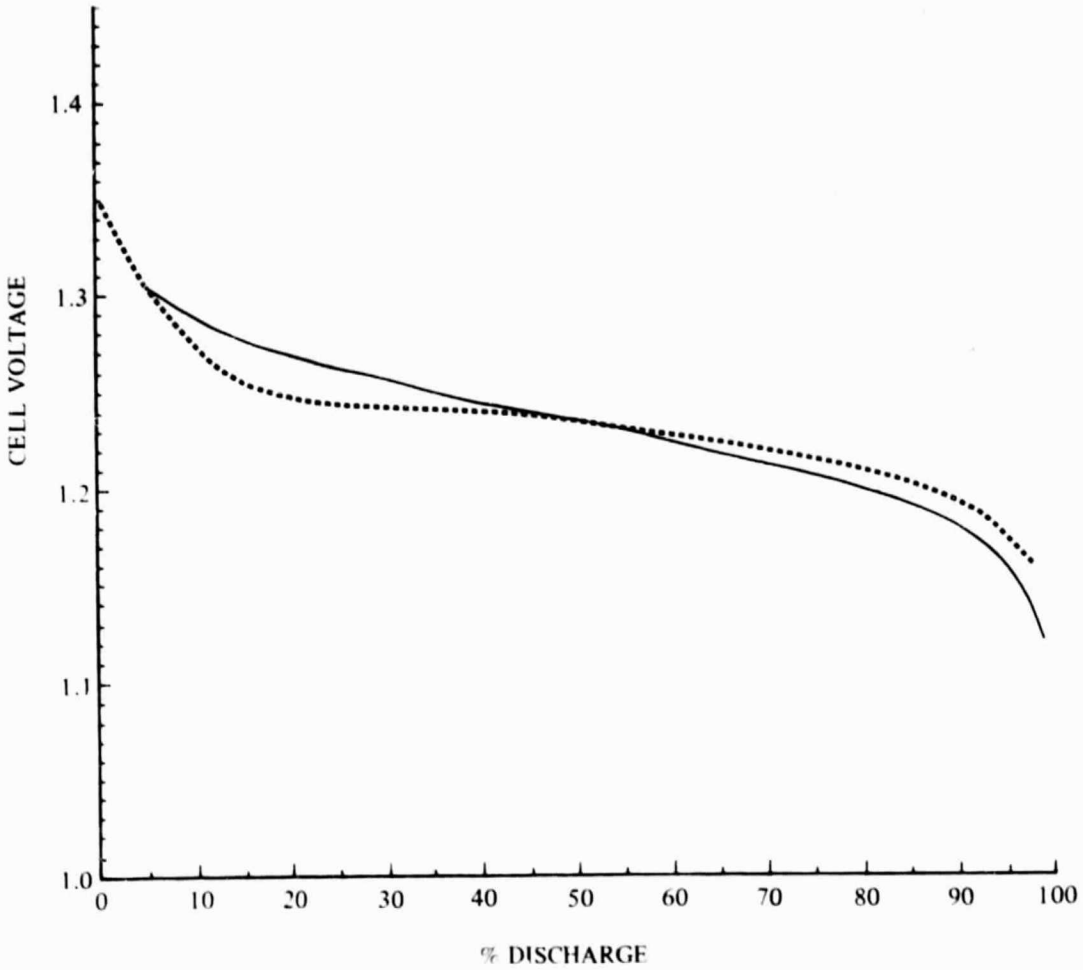

Figure 1. Calculated discharge curve based on the simple thermodynamic model, equation (7). The broken curve is experimental data.

where K = A/RT. The value of K was determined by a least squares fit using four different discharge curves obtained from the Crane data. The mean "best fit" value for K was 0.789. Thus, the discharge equation becomes

$$E = 1.294 + \frac{RT}{F} \ell n \left(\frac{1-X}{X}\right) + 0.789 \frac{RT}{F} (2X-1) - i R_0 \qquad (9)$$

A calculated discharge curve based on equation 9 is shown in Figure 2. As before, an experimental curve is included for comparison. It is immediately apparent that the calculated curve is in much closer agreement with the experimental curve than is that of Model I. The effect of different values of current and temperature using equation 9 is shown in Figure 3.

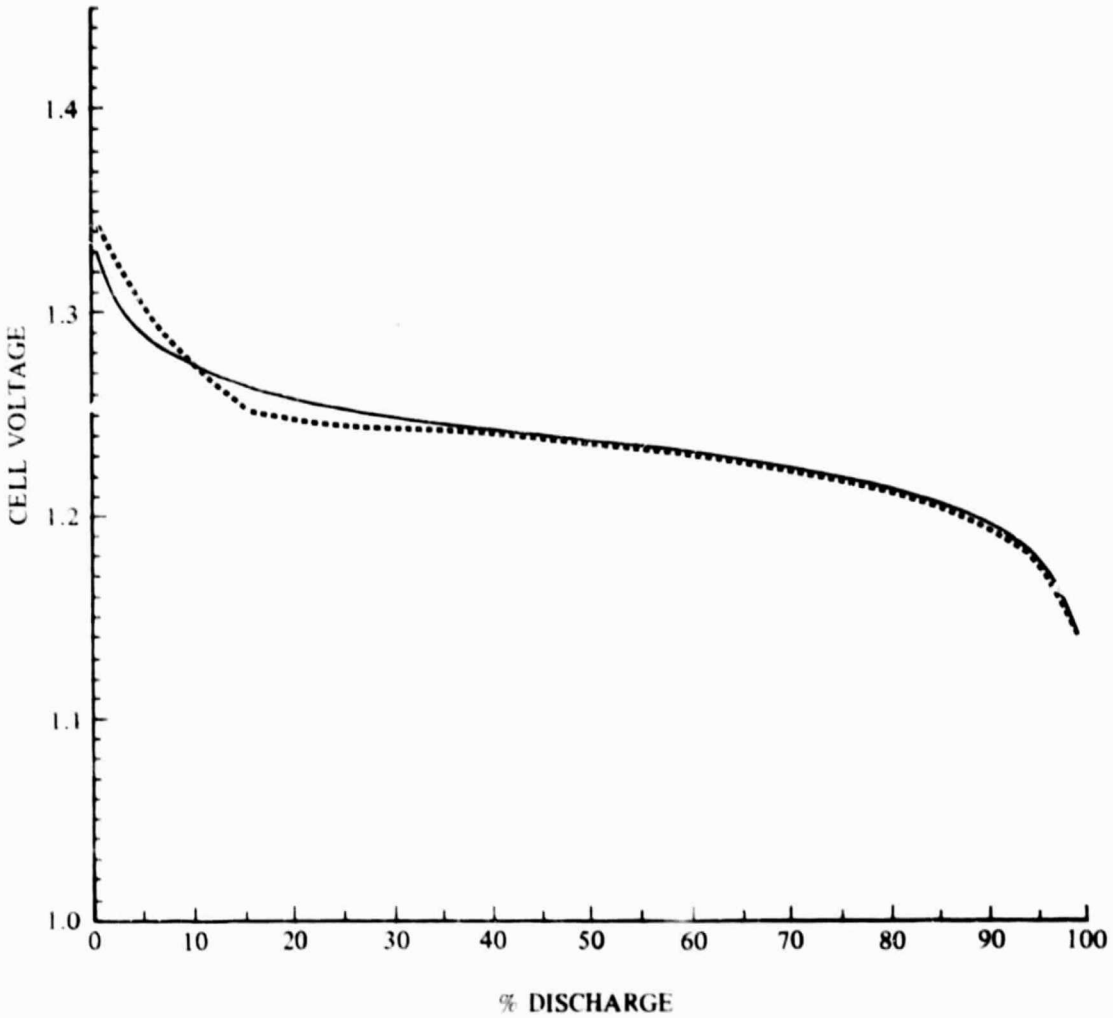

Figure 2. Calculated discharge curve based on the modified thermodynamic model, equation (9). The broken curve is experimental data.

MODEL III. MODIFIED THERMODYNAMIC MODEL WITH VARYING RESISTANCE

In the previous model it was assumed that the cell resistance remains constant throughout the discharge. However, it has been shown that $Ni(OH)_2$ in the pure state is a poorly conducting p-type semiconductor (6-9). On charging, n-type conductivity can be developed (8). It seems reasonable that the cell resistance would vary with the extent of discharge, reaching the lowest resistance when fully charged and the highest resistance when fully discharged. To this end, it was assumed *a priori* that the resistance takes the form $R = R_o e^{-(1-x)}$ where X is the fraction of discharge. Thus R_o represents the cell resistance when fully discharged. The discharge equation then becomes

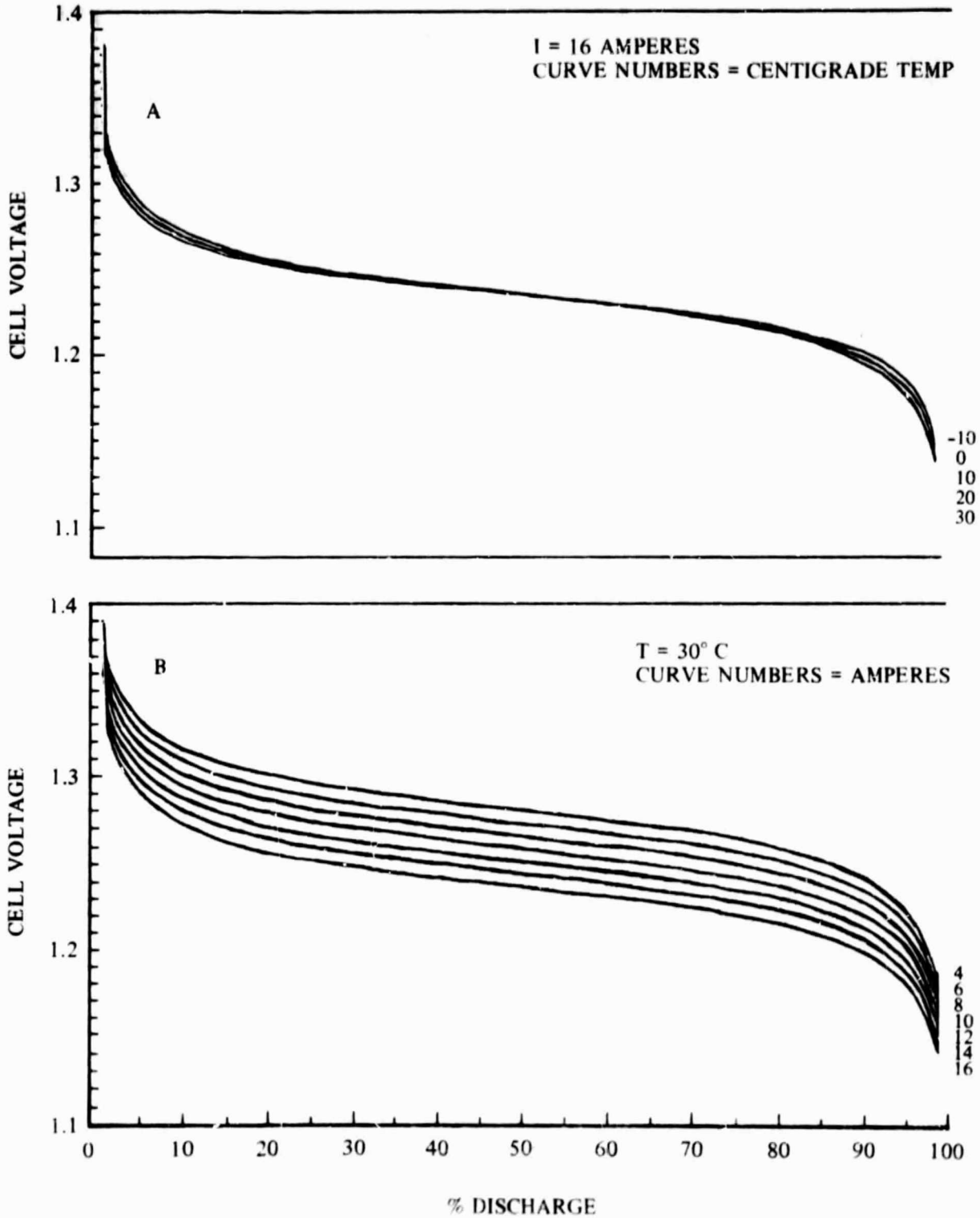

Figure 3. Effect of temperature (A) and current (B) on discharge curve. Curves are based on model II.

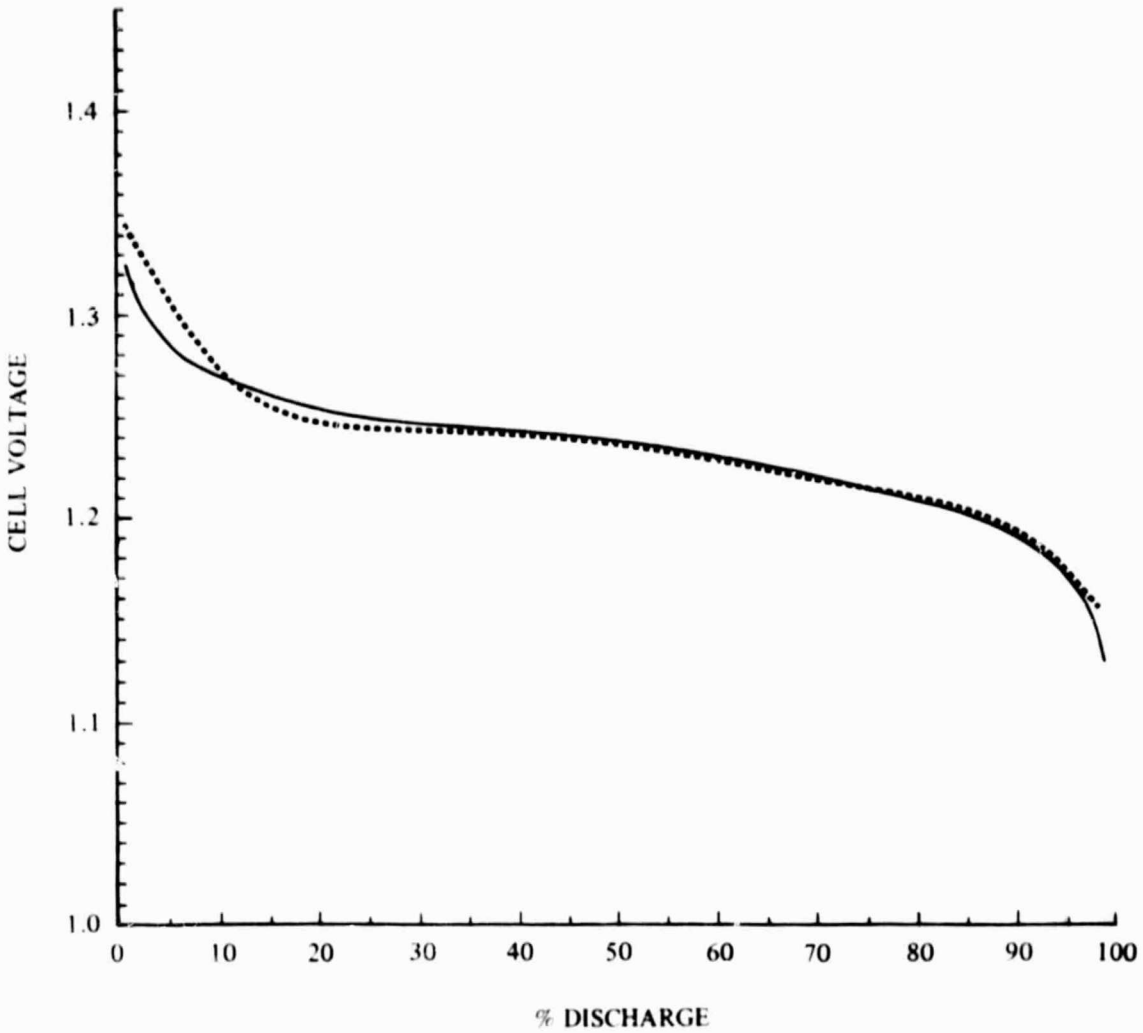

Figure 4. Calculated discharge curve based on Model III, equation (10). The broken curve is experimental data.

$$E = 1.294 + \frac{RT}{F} \ln\left(\frac{1-X}{X}\right) + \frac{RT}{F} K(2X-1) - i R_0 \exp[-(1-X)] \qquad (10)$$

As before, K was treated as an adjustable parameter and evaluated by a least squares fit. The mean "best fit" K = 1.973. The calculated discharge curve based on equation 10 is shown in Figure 4. As before, an experimental curve is included for comparison.

MODEL IV. CHRONOPOTENTIOMETRIC MODEL

"Chronopotentiometry" refers to an experimental technique in which electrolysis is carried out at controlled current and the potential is monitored as a function of time (10). The simples. and most common approach involves electrolysis at constant current. Under these conditions, the electrolysis reaction proceeds at a constant rate. If the reaction at one of the electrodes is the limiting factor, i.e. if one electrode is much smaller or if it has much less electroactive material available, then the shape of the potential-time curve will depend primarily on the reactions at that electrode. The potential assumes values characteristic of the redox couple and varies with time as the oxidized/reduced concentration ratio changes at the electrode surface. Eventually, after the concentration of reactant drops to zero at the electrode surface its flux is insufficient to consume all of the electrons which cross the electrode-solution interface. In the case of a reduction, the potential will then rapidly shift toward more negative values until a new second reduction process can start. The time required for this potential transition to occur is called τ, the transition time. A typical chronopotentiogram is shown in Figure 5.

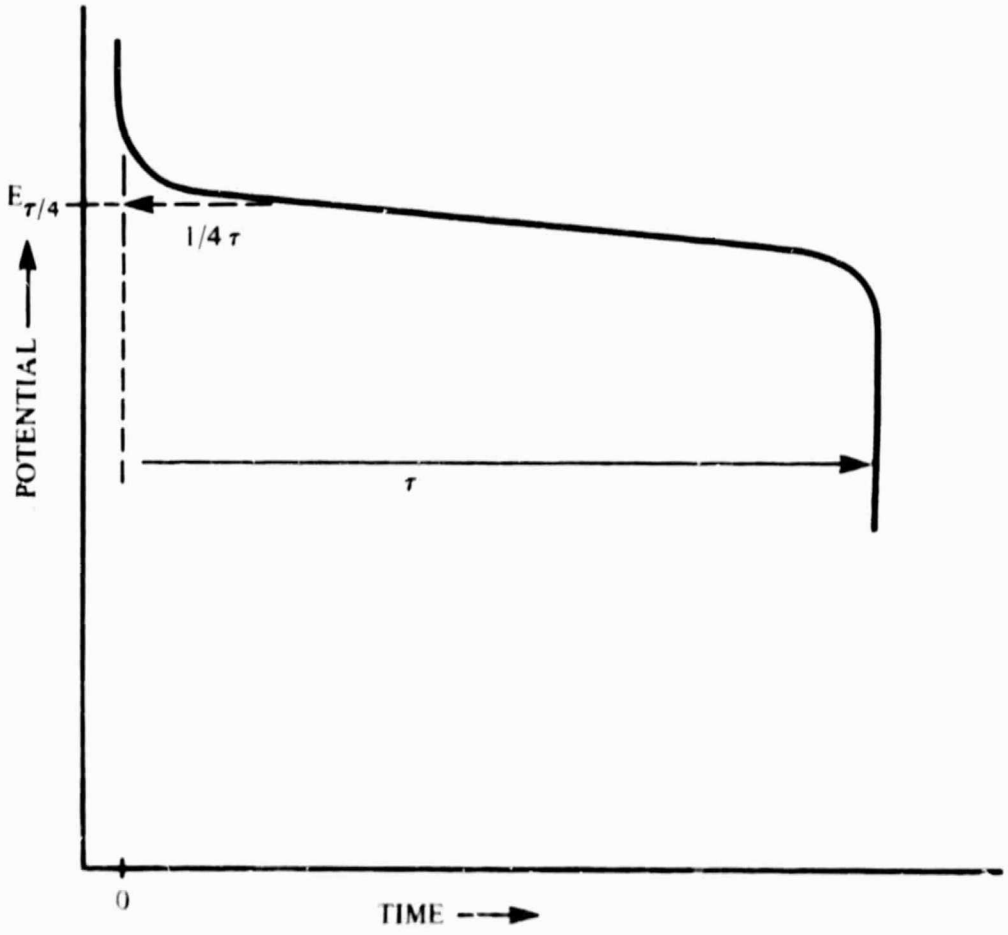

Figure 5. A typical chronopotentiogram. The quarter-wave potential, $E_{\tau/4}$, corresponds to the potential at a time $t = 1/4\ \tau$.

If electron transfer is rapid, the Nernst equation applies. It can be shown (11) that the potential-time curve has the form

$$E = E_{\tau/4} + \frac{RT}{nF} \ln\left(\frac{\tau^{1/2} - t^{1/2}}{t^{1/2}}\right) \tag{11a}$$

Rearranging the terms within the logarithm one obtains

$$E = E_{\tau/4} + \frac{RT}{nF} \ln\left[\frac{1 - \left(\frac{t}{\tau}\right)^{1/2}}{\left(\frac{t}{\tau}\right)^{1/2}}\right] \tag{11b}$$

Since electrolysis is being carried out at constant current the amount of charge passed at any time, t, after the start of electrolysis is given by the current time product, $q = it$. In addition, the charge corresponding to the total capacity of the electrode is given by the current and the transition time, $Q = i\tau$. Thus, the fraction discharged $X = q/Q = t/\tau$. In addition, $E_{\tau/4} \approx E^{o'}$ (11). Then the discharge equation is

$$E = 1.294 + \frac{RT}{F} \ln\left(\frac{1-X^{1/2}}{X^{1/2}}\right) - i R_0 \tag{12}$$

A calculated discharge curve based on equation 12 is shown in Figure 6. An experimental curve is included for comparison.

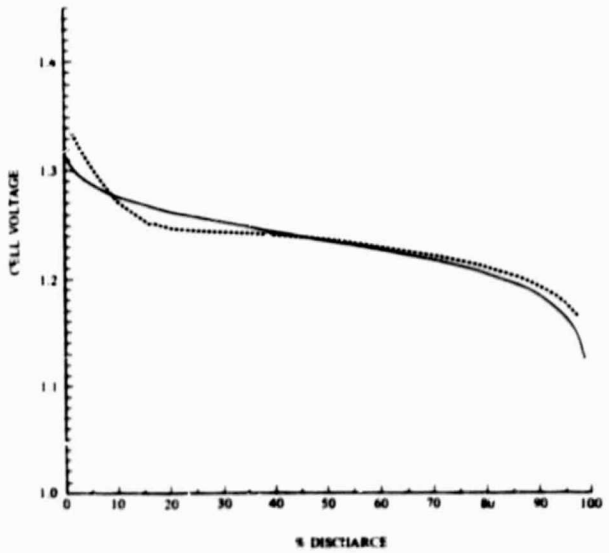

Figure 6. Calculated discharge curve based on Model IV, equation (12). The broken curve is experimental data.

MODEL V. MODIFIED CHRONOPOTENTIOMETRIC MODEL

In the normal chronopotentiometry experiment the current is held constant thus forcing reaction to occur at a fixed rate. The presence of a finite capacitance, which might arise from the double layer at the electrode-solution interface or within the deposit of active material, introduces a non-faradaic charging current, i_c, proportional to dE/dt. Thus, only a portion, i_f, of the total current goes to the faradaic reaction

$$i = i_f + i_c \tag{13}$$

Even though i is constant, i_c and i_f vary with time. This effect leads to a distortion of the potential-time curve. de Vries (12) has shown that the charging contribution is represented by the dimensionless parameter

$$K = \left(\frac{RT}{nF}\right)\frac{C_d}{nFC_0^*(\pi D\tau)^{1/2}} \tag{14a}$$

where C_d is the capacitance, C_o^* the bulk concentration and D the diffusion coefficient. Also

$$i_f \tau^{1/2} = \frac{n F A D^{1/2} \pi^{1/2} C_0^*}{2} \tag{14b}$$

which is known as the Sand equation (13). Rearranging equation 14a one obtains

$$n F D^{1/2} \pi^{1/2} C_0^* = \frac{RT}{nF}\frac{C_d}{K\tau^{1/2}} \tag{14c}$$

and from equation 14b

$$\frac{2 i_f \tau^{1/2}}{A} = n F D^{1/2} \pi^{1/2} C_0^* \tag{14d}$$

Then,

$$\frac{2 i_f \tau^{1/2}}{A} = \frac{RT}{nF}\frac{C_d}{K\tau^{1/2}} \tag{14e}$$

Solving for $1/\tau$,

$$\frac{1}{\tau} = \left(\frac{2nF}{RT}\right)\left(\frac{K}{C_d A}\right) i_f \tag{14f}$$

and

$$\frac{t}{\tau} = \left(\frac{2nF}{RT}\right)\left(\frac{K}{C_d A}\right) i_f t = \left(\frac{2nF}{RT}\right)\left(\frac{K}{C_d A}\right) X \tag{15}$$

where $X = i_f t$ is the fraction of discharge. Substituting equation 15 into equation 12 and letting $(K/C_d A) = K$ one obtains

$$E = 1.294 + \frac{RT}{F} \ln \left[\frac{1 - \left(\frac{2nF}{RT} K X\right)^{1/2}}{\left(\frac{2nF}{RT} K X\right)^{1/2}}\right] - i R_0 \tag{16}$$

The value of K was evaluated by a least squares fit of the experimental discharge curves. The mean best fit value for K was 0.01208. The equation for the discharge curve then becomes

$$E = 1.294 + \frac{RT}{F} \ln \left[\frac{1 - \left(0.02416 \frac{F}{RT} X\right)^{1/2}}{\left(0.02416 \frac{F}{RT} X\right)^{1/2}}\right] - i R_0 \tag{17}$$

The calculated discharge curve based on equation 17 is shown in Figure 7.

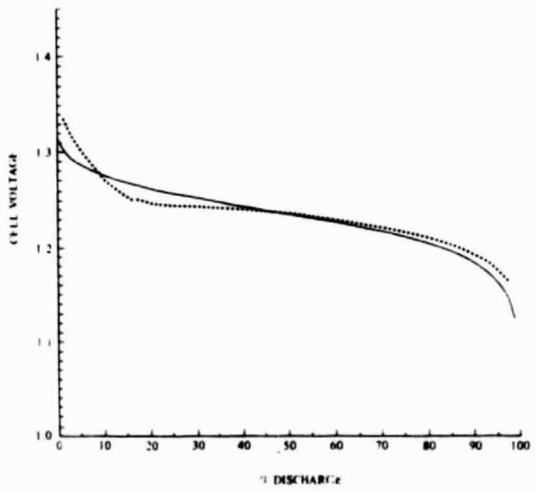

Figure 7. Calculated discharge curve based on Model V, equation (17). The broken curve is experimental data.

COMPARISON OF THE MODELS

The equations corresponding to the models discussed in this report are summarized in Table 1.

For each model, an error distribution was calculated with respect to each of the four experimental discharge curves. A typical set of error curves is shown in Figure 8. A summary of the respective standard deviations is shown in Table 2. As might be expected, Model I is in poor agreement with the experimental data (see Figure 1, Figure 8 and Table 2). None of the calculated discharge curves is in complete agreement with experiment for the full discharge. For Models II, III IV and V, agreement seems quite good for 50-100% discharge (see Figures 2, 4-8 and Table 2). Standard deviations calculated for the full curve, 0-50% discharge and 50-100% discharge are included in Table 2. In each case, however, agreement is poorest in the initial portion of the discharge curve.

Table 1. Summary of Equations for the Five Models

Model	Equation[a]
I Simple Thermodynamic	$E = 1.294 + \frac{RT}{nF} \ln\left(\frac{1-X}{X}\right) - i R_0$
II Modified Thermodynamic	$E = 1.294 + \frac{RT}{nF} \ln\left(\frac{1-X}{X}\right) + 0.789 \frac{RT}{nF}(2X-1) - i R_0$
III Modified Thermodynamic with Varying Resistance	$E = 1.294 + \frac{RT}{nF} \ln\left(\frac{1-X}{X}\right) + 1.973 \frac{RT}{nF}(2X-1) - i R_0 e^{-(1-X)}$
IV Chronopotentiometric	$E = 1.294 + \frac{RT}{nF} \ln\left(\frac{1-X^{1/2}}{X^{1/2}}\right) - i R_0$
V Modified Chronopotentiometric	$E = 1.294 + \frac{RT}{nF} \ln\left[\frac{1-\left(.01208 \frac{2nF}{RT} X\right)^{1/2}}{\left(.01208 \frac{2nF}{RT} X\right)^{1/2}}\right] - i R_0$

[a] X is the fraction of discharge, R_0 is the cell resistance

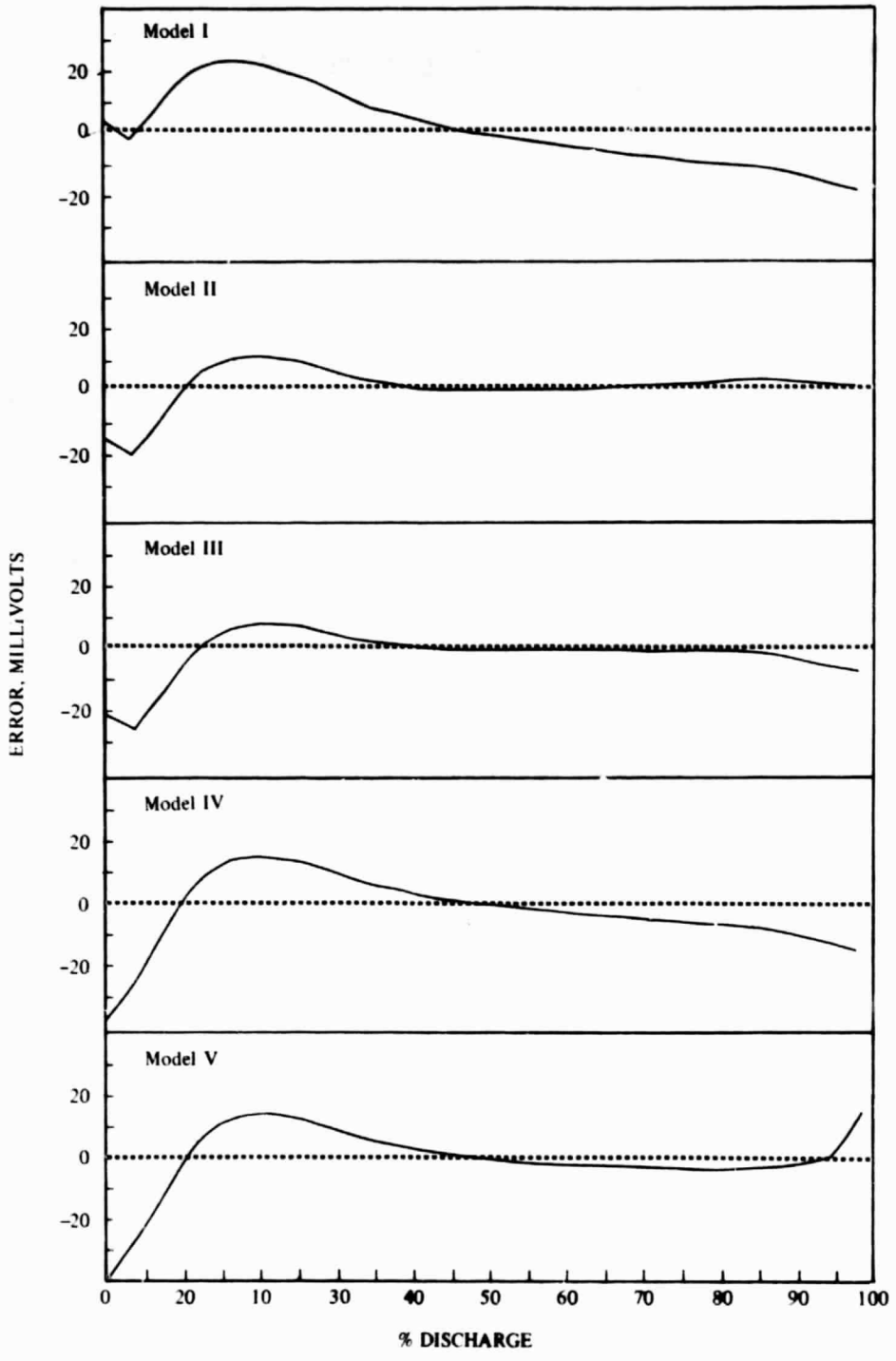

Figure 8. Typical error curves for the five models.
The curves shown are all with respect to the same experimental discharge.

Table 2. Comparison of Errors for the Models

Model[a]	Standard Deviation[b], millivolts		
	0–100%	0-50%	50-100%
I	14.4	13.9	14.8
II	8.1	9.5	5.7
III	9.7	11.1	7.6
IV	13.2	14.0	12.0
V	10.8	14.0	6.4

[a]Correspond to the equations listed in Table 1.

[b]Each standard deviation is the mean for the four experimental discharge curves

None of the models accurately represent the initial portion of experimental discharge curves. The disagreement may be the result of an artifact in the experimental procedure used to collect the discharge data or perhaps the models neglect some fundamental process which occurs in the early stages of discharge. This problem certainly warrants further investigation.

Models II and III appear to agree more closely with experiment than do the others. Best agreement in all regions of the discharge curve is found with Model II.